Peer-reviewed version available at *Energies* **2018**, *11*, 36; doi:10.3390/en11010036

Article

A Novel High Accuracy PV Cell Model Including Selfheating and Parameter Variation

Aurel Gontean[1,*], Septimiu Lica[1], Szilard Bularka[1], Roland Szabo[1] and Dan Lascu[1]

[1] Politehnica University Timisoara, Romania; aurel.gontean@upt.ro
* Correspondence: aurel.gontean@upt.ro; Tel.: +40-745-121-383

Abstract: This paper proposes a novel model for a PV cell with parameters variance dependency on temperature and irradiance included. The model relies on commercial available data, calculates the cell parameters for standard conditions and then extrapolates them for the whole operating range. An up-to-date review of the PV modeling is also included with series and parallel parasitic resistance values and dependencies discussed. The parameters variance is analyzed and included in the proposed PV model, where the self-heating phenomenon is also considered. Each parameter variance is compared to the results from different authors. The model includes only standard components and can be run on any SPICE-based simulator. Unlike other approaches that consider the internal temperature as a parameter, our proposal relies on air temperature as an input and computes the actual internal temperature accordingly. Finally, the model is validated via experiments and comparisons to similar approaches are provided.

Keywords: PV cell; model; simulation; SPICE; selfheating; parameters variation

---

1. Introduction

PV cells have been extensively studied in the last decades [1-8] as solar energy is more and more accepted as a viable alternative to traditional energy sources. Modeling the PV behavior is useful for system design, planning, research and training. The goal of this work is to develop an accurate model for a PV Cell, expandable to a whole module, using affordable tools and taking into account parameters variations. LTSpice [9] was chosen as the simulation tool due to its free cost and wide acceptance, Visual Studio Express [10], also a free tool, was used for parameters estimation and solution validation. Finally, S-Math Studio [11] was selected for the trial and error different evaluations. The solution implies a reasonable computing power and provides fast convergence. The model itself is portable, as it uses only standard components and is also vendor independent. The input data is usually provided from the manufacturer's datasheet or can be obtained via experiments.

Unlike other approaches, the model input temperature is the ambient/air temperature, and based on actual irradiance the model calculates the internal (silicon) temperature and provides the actual I-V and P-V curves.

The paper is organized as follows: Section 2 briefly analyzes the classical PV model and its equations. Section 3 deals with the information provided by the PV cell datasheet and the equipment involved in measurements. Finding the solution for the PV cell model is analyzed in section 4, with section 4.1 introducing the solving algorithm. A review of parameters variation is the subject for Section 4.2, including the real operating conditions, when the PV solar cell is selfheating. The new PV cell model is proposed in Section 4.3, the experimental results are exposed in Section 5, while conclusions are presented in Section 6.

2. The Classical PV Cell Model

The equivalent circuit of a solar cell is investigated in several prior works [12 – 38]. It is generally accepted that a PV cell can be modeled by the circuit in Figure 1, including one [12 - 32], two [33 – 35] and rarely three or more diodes [36 - 37].

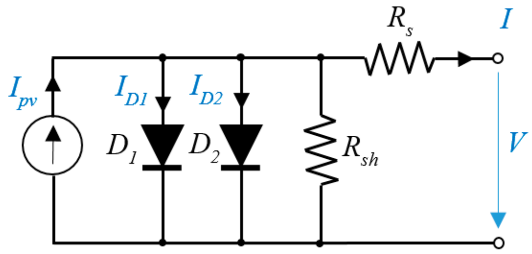

Figure 1. Equivalent circuit of a photovoltaic cell.

In Figure 1, I_{pv} current source models the photo generated current, with a linear dependency on the irradiance. The first diode, D_1, is associated with the diffusion mechanism. The second diode, D_2, is inserted to include the effect of charge recombination. Resistance R_s represents the cell series resistance and resistance R_{sh} the cell parallel (shunt) resistance. Resistance R_s is related to losses in cell solder bonds, wires, junctions and so on and it is usually bellow 1Ω. Resistance R_{sh} is related to the leakage current through the high conductivity shunts across the p-n junction and is usually in the order of ten of ohms to several kΩ. The circuit in Figure 1 can be extended to any combination of n_s series – n_p parallel cells within a PV module (array). In this paper we shall consider only one diode in the model, D_1, neglecting D_2. The equations will be provided in a general form, while the simulations and experiments will be conducted for a single cell, that is for $n_s = n_p = 1$.

Referring to Figure 1, according to Kirchhoff's current law (KCL), one can write:

$$I = I_{pv} - I_{01}\left\{\exp\left[\frac{q(V + IR_s)}{a_1 n_s kT}\right] - 1\right\} - \frac{V + IR_s}{R_{sh}} \tag{1}$$

where I_{01} is the diode reverse saturation current, q is the electron charge, k is the Boltzmann constant, T is the actual silicon temperature and a_1 is the ideality factor of the diode.

Current I_{pv} linearly depends on irradiation and temperature [15], [18]:

$$I_{pv} = \left(I_{pv,ref} + k_I \Delta T\right)\frac{G}{G_{ref}} \tag{2}$$

At the maximum power point, using (1), the maximum power P_{mp} can be derived [22]:

$$P_{mp} = V_{mp} I_{mp} = V_{mp}\left\{I_{pv} - I_{01}\left[exp\left(\frac{q}{kT}\frac{V_{mp} + I_{mp}R_s}{a_1 n_s}\right) - 1\right] - \frac{V_{mp} + I_{mp}R_s}{R_{sh}}\right\} \tag{3}$$

Even in (1) and (3) I_{pv} is considered equal to I_{sc}, a more accurate formula for I_{pv} is [22]:

$$I_{pv,ref} = \frac{R_{sh} + R_s}{R_{sh}} I_{sc,ref} \tag{4}$$

A good overview of the PV cell performance can be found in [12], where an empirical formula for the fill factor FF is introduced, considering the single diode model:

$$FF = \frac{\frac{qV_{0c}}{a_1 n_s kT} - \ln\left(0.72 + \frac{qV_{0c}}{a_1 n_s kT}\right)}{\frac{qV_{0c}}{a_1 n_s kT} + 1} \tag{5}$$

Peer-reviewed version available at Energies 2018, 11, 36; doi:10.3390/en11010036

3. Materials, Methods and Equipment

For our experiments we have chosen a high efficiency low cost monocrystalline Silicon PV solar cell, unmounted in panels [39]. The datasheet of the PV cell offers a limited amount of data, summarized in Table 1.

Table 1. PV Cell main specifications on STC (1000W/m^2, AM 1.5, 25°C)

Symbol	Description	Value
$V_{oc,cell,ref}$	Cell open circuit voltage	0.699 V
$I_{sc,ref}$	Short circuit current	9.206 A
V_{mp}	Maximum power voltage	0.572 V
I_{mp}	Maximum power current	8.756 A
(P_{mp})	Maximum power $P_{mp} = V_{mp} I_{mp}$	(5.21 W)
FF	Fill factor	(81.90%)
k_I	Short circuit temperature coefficient	0.035 %/K
k_V	Open circuit voltage temperature coefficient	-0.25 %/K
k_P	Maximum power temperature coefficient	-0.41 %/K

It is important to note that $V_{mp} = (0.75 \ldots 0.9) \cdot V_{oc}$ for any solar cell. This is a good starting point for any simulation or MPPT algorithm implementation.

The data from the datasheet is confusing, as:

1. The claimed maximum power (5.21W) differs from $V_{mp} I_{mp} = 5.01$W. This latter value will be considered subsequently.
2. The claimed fill factor (81.90%) differs from the standard definition $FF = \frac{V_{mp} \cdot I_{mp}}{V_{oc,ref} \cdot I_{oc,ref}} = 77.82\%$

The empirical equation (5) yields an approximate result ($FF \cong 84.08\%$) when compared to the datasheet values (Table 1).

The irradiance was measured with a Klipp and Zonen SHP1 pyrheliometer with integrated temperature sensor for temperature compensation. The internal silicon temperature was determined with a FLIR E8 infrared camera and a PT1000 temperature sensor on the rear of the PV cell. In order to obtain reliable data, the PT1000 temperature sensor was glued with high thermally conductive adhesive to the backside metal coating of the PV cell. The ambient temperature was measured using the National Instruments NI USB T01 interface. Due to the extremely low internal series resistance R_s, several series cells were carefully wired and a Kelvin connection had to be used for voltage measurements. The measurements were performed under real life conditions, when the solar irradiance was maximum with the PV cells oriented toward the sun on 45 degree inclined support. The load was an ET Instrument ESL-Solar, configured in MPPT mode.

4. Classical Model Solving

Several ways for solving the equations have been proposed [17, 20, 22, 26, 27, 28, 30, 32]. One of the difficulties is the implicit nature of equation (1) regarding I. This has been addressed by various techniques, ranging from pure mathematical approaches (including Lambertian W-Function, [31]) to pure numerical solutions, mainly in MATLAB [5, 6, 16, 35]. Later models [40 - 52] take into account the parameters variation with temperature and irradiance. However the most common approach considers the internal PV temperature as an independent parameter and plots the I-V family curves for different temperatures. This aspect will be covered in the subsequent sections. It has to be stressed out that the exponential nature of equation (1) determines that a small variation in any of the terms involved in the exponential term to substantially modify the final result. This aspect will be addressed in sections 5 and 6.

Preprints (www.preprints.org) | NOT PEER-REVIEWED | Posted: 7 December 2017 doi:10.20944/preprints201712.0040.v1

Peer-reviewed version available at *Energies* **2018**, *11*, 36; doi:10.3390/en11010036

4.1. Solving the Equations for the Classical PV Model

The method introduced here is an extension of the method proposed by Villalva et al. [22] and involves the following steps:

1. Compute a_1
2. For validation purposes determine the limits $R_{s,max}$ and $R_{sh,min}$
3. For all values between $[0, R_{s,max}]$ with $R_{s,inc}$ as increment, numerically solve (1) for the MPP.
4. When the maximum power error is below the imposed threshold error, R_s is established and R_{sh} can be computed.

A VB.net application has been developed by the authors in order to numerically solve and compute the model parameters. The application can be downloaded from http://tess.upt.ro. Figure 2 depicts a print screen for the initial parameter passing (a) and the results (b).

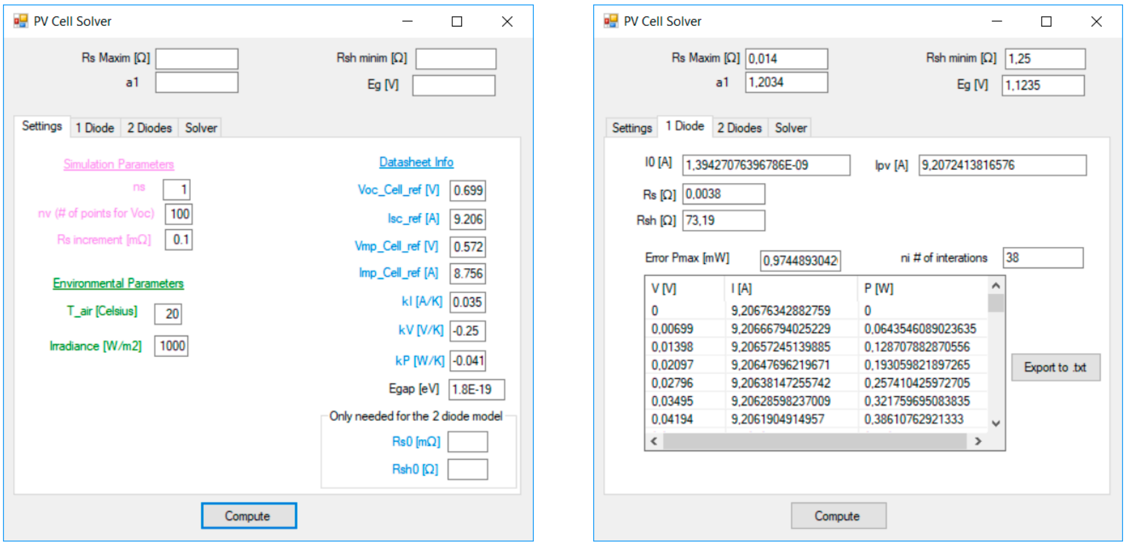

(**a**) (**b**)

Figure 2. VB.net PV Cell solver: (**a**) Entering parameters values; (**b**) Getting the solution.

In our case, using the values taken from the datasheet for $n_s = n_p = 1$, it results that:

$$R_{s,max} = \frac{V_{0c} - V_{mp}}{I_{mp}} = 14\ m\Omega \tag{6}$$

$$R_{p,min} = \frac{V_{mp}}{I_{sc,ref} - I_{mp}} - R_{s,max} = 1.25\ \Omega \tag{7}$$

These limits are important to set reliable ranges for the algorithm. The final results are listed in Table 2.

Table 2. Vb.net application results

Symbol	Description	Results
$\boldsymbol{I_{pv,ref}}$	Photo generated current	9.207 A
$\boldsymbol{I_{o,ref}}$	Reverse diode current	1.39427 nA
$\boldsymbol{R_{s,max}}$	Maximum Rs value (initial guess)	14 mΩ
$\boldsymbol{R_{s,ref}}$	Series resistance	3.8 mΩ
$\boldsymbol{R_{sh,min}}$	Minimum Rsh value (initial guess)	1.25 Ω
$\boldsymbol{R_{sh,ref}}$	Parallel resistance	73.19 Ω
$\boldsymbol{a_{1,ref}}$	Ideality factor	1.2034
$\boldsymbol{E_{g,ref}}$	Bandgap energy	1.795E-19 eV
$\boldsymbol{V_{g,ref}}$	Bandgap voltage	1.121 V

Preprints (www.preprints.org) | NOT PEER-REVIEWED | Posted: 7 December 2017 doi:10.20944/preprints201712.0040.v1

Peer-reviewed version available at *Energies* **2018**, *11*, 36; doi:10.3390/en11010036

Several attempts have been made for finding explicit expressions for R_s and R_{sh} based on actual datasheet data. For example, Cubas et al. [31] offer the R_{sh} formula (with R_s as an argument, considering $n_s = 1$):

$$R_{sh} = \frac{\left(V_{mp} - I_{mp}R_s\right)\left[V_{mp} - R_s\left(I_{sc} - I_{mp}\right) - \frac{a_1 kT}{q}\right]}{\left(V_{mp} - I_{mp}R_s\right)\left(I_{sc} - I_{mp}\right) - \frac{a_1 kT I_{mp}}{q}} \quad (8)$$

For the above data, the R_{sh} formula (8) yields a result of 59.43 Ω, compared to the actual value of 73.19 Ω.

In a simplified model ($R_{sh} \to \infty$), Xiao et al. [18] propose for R_s the following relationship (again $n_s = 1$):

$$R_s = \frac{\frac{a_1 kT}{q} ln\left[\left(1 - \frac{I_{mp}}{I_{ph}}\right) exp\left(\frac{qV_{0c}}{a_1 kT}\right) + \frac{I_{mp}}{I_{ph}}\right] - V_{mp}}{I_{mp}} \quad (9)$$

Here (9) yields $R_s = 0.7m\Omega$, quite far from its actual value (3.8 mΩ).

4.2. Parameters variation for different conditions

The parameters in equations (1) – (4) are not constant over the environmental conditions, as $I_o, R_s, R_{sh}, a_i, E_g$ depend on temperature and irradiance. A brief review of these dependencies is provided bellow.

4.2.1. Diode saturation current – I_{01}

Phang et al. [13] show that if I_{pv} is below 10A, I_{01} can be derived as in (10):

$$I_{01} = \left(I_{sc} - \frac{V_{oc}}{R_{sh}}\right) exp\left(-\frac{V_{oc}}{a_1 V_T}\right) \quad (10)$$

I_{01} in (10) yields a very good result of 1.3969 nA vs 1.39427nA obtained in Table 2.

Gow and Manning [15] were among the first to claim that:

$$I_{01} = C_1 T^3 e^{-\frac{qV_g}{kT}} \quad (11)$$

The temperature dependence of this current is more detailed expressed by [16], [20]:

$$I_{01} = I_{01,ref}\left(\frac{T}{T_{25}}\right)^3 exp\left[\frac{qV_g}{ka_1}\left(\frac{1}{T_{ref}} - \frac{1}{T}\right)\right] \quad (12)$$

where V_g is the bandgap voltage of the semiconductor ($V_g = 1.1 \ldots 1.3V$ for Si at 25 °C).

$I_{01,ref}$ can be derived from (1) at the reference temperature as:

$$I_{01,ref} = \frac{I_{sc,ref}}{\exp\left(\frac{qV_{0c,ref}}{a_1 n_s kT_{ref}}\right) - 1} \quad (13)$$

According to Vilalva et al. [22], $I_{01,ref}$ can be further improved:

$$I_{01,ref} = \frac{I_{sc,ref} + k_I \Delta T}{\exp\left[\frac{q\left(V_{0c,ref} + k_V \Delta T\right)}{a_1 n_s kT}\right] - 1} \quad (14)$$

Preprints (www.preprints.org) | NOT PEER-REVIEWED | Posted: 7 December 2017 doi:10.20944/preprints201712.0040.v1

Peer-reviewed version available at Energies 2018, 11, 36; doi:10.3390/en11010036

In subchapter 4.6.3 of [8], van Zeghbroeck states an equation in which $I_{01,ref}$ can be derived from, that can offer an alternate way to estimate $I_{01,ref}$:

$$V_{mp} = V_{mp} ln \frac{1 + \frac{I_{pv}}{I_{01,ref}}}{1 + \frac{V_{mp}}{V_T}} \tag{15}$$

This proves to be not very accurate in our case, as with the values from Table 1, $I_{0,ref}$ from (15) results 0.085 nA, quite far from the actual value (1.39427 nA).

4.2.2. Band gap energy and bandgap voltage – E_g, V_g

Van Zeghbroeck [8] shows that the bandgap energy, E_g, exhibits a small temperature dependence as in (16).

$$E_g = 1.166 - \frac{0.000477 \cdot T^2}{636 + T} \tag{16}$$

From (16), $E_{g,ref} = 1.121$ eV for silicon cells at 25°C. This is the value considered in Table 1.

In contrast, Kim et al. [23] define the variance for E_g for silicon to be:

$$E_g = 1.16 - \frac{7.02 \cdot 10^{-4} \cdot T^2}{T - 1108} \tag{17}$$

Both (16) and (17) fit in the [1.1 … 1.3V] interval specified when equation (12) was introduced. In our approach shown in Figure 3, we adopted the Van Zeghbroeck proposal because it will finally lead to a more realistic value for a_1 and close to the linear approximation of E_g against temperature suggested by Radziemska and Klugmann [40], which indicate a temperature coefficient $\mathrm{d}E_g/\mathrm{d}T = -2.3 \cdot 10^{-4}\,\mathrm{eV/K}$.

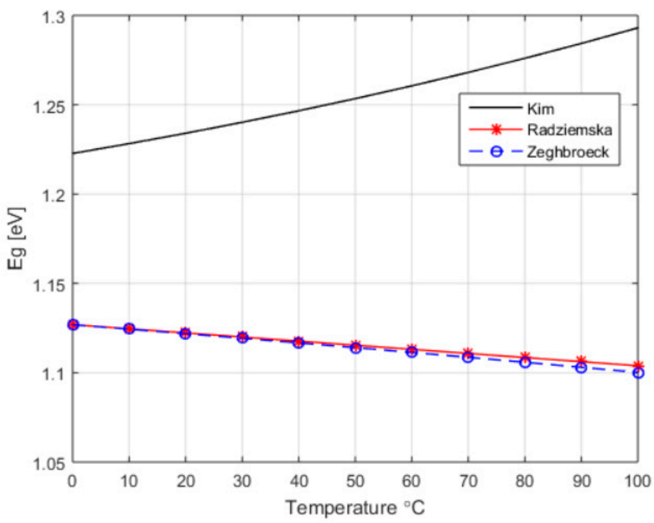

Figure 3. E_g variation against temperature according to several authors

4.2.3. Series resistance – R_s

Honsberg and Bowden [7] show that R_s does not influence V_{0c}, but close to the open-circuit voltage, the I-V curve is affected by R_s. An initial estimation for R_s is to find the slope of the I-V curve at the open-circuit voltage point (18):

$$R_{s0} = -\left.\frac{\mathrm{d}V}{\mathrm{d}I}\right|_{V=V_{0c}} \tag{18}$$

Preprints (www.preprints.org) | NOT PEER-REVIEWED | Posted: 7 December 2017 doi:10.20944/preprints201712.0040.v1

Peer-reviewed version available at Energies 2018, 11, 36; doi:10.3390/en11010036

In our case, $R_{s0} = 11$ mΩ (while $R_s = 3.8$mΩ, as it will later be shown).

Cuce and Bali [43], Cuce et al. [47] and Singh et al. [42] claim that R_s linearly decreases with the temperature. Obviously, reducing R_s yields an increase in the output current.

A PV Cell model is also available in MATLAB Simscape [52]. It consists of the same circuit as in Figure 1, where the user can choose between:

- An 8-parameter model, where equation (1) describes the output current
- A 5-parameter model that neglects D_2 in Figure 1 and the value of the shunt resistor is infinite.

Both models adjust the resistance values and current parameters as a function of temperature. Resistance R_s is assumed to be given by (19):

$$R_s = R_{s,ref}\left(\frac{T}{T_{ref}}\right)^{k'_{Rs}} \tag{19}$$

where k'_{Rs} is the temperature exponent for R_s. k'_{Rs} is 0 by default and when modified has to be positive.

Figure 4 summarizes all these above dependencies. In order to have the results in the same range, Cubas et al. [31] and Cuce et al. [47] results were scaled, and equation (19) was re-written as in (20), interchanging T with T_{ref} and k_{Rs} was estimated as 4.9 for the best fit. A linear dependency is easy to implement, but might also lead to results not physically true (for example Cuce et al. [47] data lead to negative R_s resistances for temperatures over 75°C and so does Cubas et al. [31] over 97°C).

$$R_s = R_{s,ref}\left(\frac{T_{ref}}{T}\right)^{k_{Rs}} \tag{20}$$

where $|k'_{Rs}| = |k'_{Rs}|$.

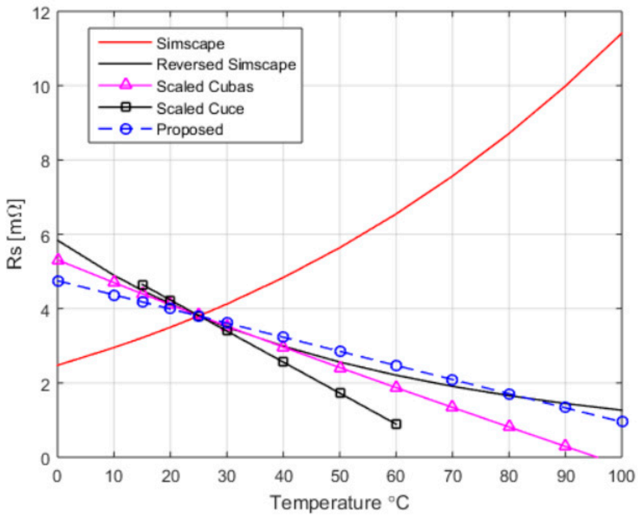

Figure 4. R_s variation against temperature by several authors

The linear law (21) was adopted for R_s and we chose $\alpha_{Rs} = -0.01\text{K}^{-1}$, again for the best fit.

$$R_s = R_{s,ref}\left[1 + \alpha_{Rs}\left(T - T_{ref}\right)\right] \tag{21}$$

Preprints (www.preprints.org) | NOT PEER-REVIEWED | Posted: 7 December 2017 doi:10.20944/preprints201712.0040.v1

Peer-reviewed version available at *Energies* **2018**, *11*, 36; doi:10.3390/en11010036

4.2.4. Parallel resistance – R_{sh}

Honsberg and Bowden [7] and Jung and Ahmed [25] showed that the shunt resistance of a solar cell can be determined from the slope of the I-V curve close to the short-circuit point, yielding a fair approximation for R_{sh}:

$$R_{sh0} = -\left.\frac{\mathrm{d}V}{\mathrm{d}I}\right|_{I=I_{sc}} \tag{22}$$

From Figure 11.a, $R_{sh0} = 73.18\ \Omega$, very close to the accurate solution $R_{sh} = 73.19\ \Omega$, as it will later be illustrated.

Cuce and Bali [43] and Cuce et al. [47] claim that the shunt resistance linearly decreases with temperature. They explain this decrease in terms of a combination of tunneling and trapping–detrapping of the carriers through the defect states in the space-charge region of the device. These defect states act either as recombination centers or as traps depending upon the relative capture cross sections of the electrons and holes for the defect. Temperature dependency for R_{sh} is however more complicate.

R_{sh} is again modeled in MATLAB Simscape like (23):

$$R_{sh} = R_{sh,ref}\left(\frac{T}{T_{ref}}\right)^{k'_{Rsh}} \tag{23}$$

where k'_{Rsh} is the temperature exponent for R_{sh}. k'_{Rsh} is 0 by default and when modified has to be positive.

Figure 5 summarizes all these R_{sh} equations. In order to bring the results in the same range, Cubas et al. [31] and Cuce et al. [47 Cuce] dependencies were scaled, and equation (23) was re-written as in (24) interchanging T with T_{ref} and k_{Rsh} was estimated as 8 for best fit.

$$R_{sh} = R_{sh,ref}\left(\frac{T_{ref}}{T}\right)^{k_{Rsh}} \tag{24}$$

where $|k'_{Rsh}| = |k'_{Rsh}|$.

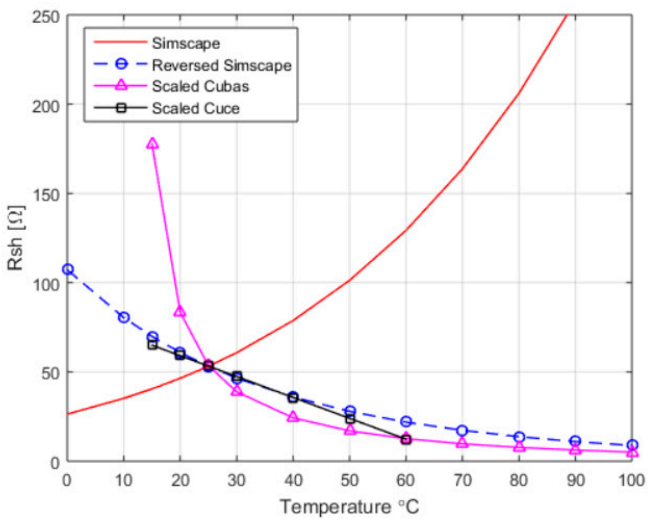

Figure 5. R_{sh} variation over temperature by several authors

Although R_{sh} influence is small in the overall model, for an accurate modeling and especially for larger temperature ranges R_{sh} linear variation is not realistic. Therefore in our model described by (24) we chose $k_{Rsh} = 8$.

Preprints (www.preprints.org) | NOT PEER-REVIEWED | Posted: 7 December 2017 doi:10.20944/preprints201712.0040.v1

Peer-reviewed version available at *Energies* **2018**, *11*, 36; doi:10.3390/en11010036

4.2.5. Ideality diode factor – a_1

Some authors consider the ideality factor as being constant over the operating temperature range and with a generic value for a_1 in the interval [1, 1.5] for every kind of cell [22], [31]. Cuce et al. [29] propose $a_1 = 1.2$ for monocrystalline silicon cells, and $a_1 = 1.3$ for polycrystalline ones. Some studies indicate a linear decreasing with temperature [18]. Cubas et al. [31] say that "the lack of accuracy produced when considering the ideality factor as constant is generally reduced, given that variations of this parameter only affects the curvature of the *I-V* curve." This is arguable, as a_1 interferes in an exponential dependency and small variations of a_1 lead to significant changes in $I_{01,}$and finally in I. One might say that picking a random a_1 in the above specified range will be balanced by a different I_0 , so only the pair (I_0, a_1) matters. However this approach is misleading, as it may induce impossible physical solutions.

Phang et al. [13] have the following proposal:

$$a_1 = \frac{q\left(V_{mp} + I_{mp}R_{s0} - V_{0c}\right)}{kT_{ref}\left[ln\left(\frac{I_{sc} - \frac{V_{mp}}{R_{sh0}} - I_{mp}}{I_{sc} - \frac{V_{0c}}{R_{sh}}}\right) + \frac{I_{mp}}{I_{sc} - \frac{V_{0c}}{R_{sh0}}}\right]} \tag{25}$$

De Blas et al. [17] suggest that:

$$a_1 = \frac{q\left(V_{mp} + I_{mp}R_s - V_{0c}\right)}{kT_{ref}ln\left[\frac{I_{sc} - I_{mp}\left(1 + \frac{R_s}{R_{sh}}\right) - \frac{V_{mp}}{R_{sh}}}{I_{sc}\left(1 + \frac{R_s}{R_{sh}}\right) - \frac{V_{0c}}{R_{sh}}}\right]} \tag{26}$$

E. Saloux et al. [28] somehow simplify (26) as below:

$$a_1 = \frac{q\left(V_{mp} - V_{0c}\right)}{kT_{ref}ln\left(1 - \frac{I_{mp}}{I_{sc}}\right)} \tag{27}$$

In the algorithm of Villalva [53], a different formula is introduced. Considering that for crystalline silicon $E_g = 1.8$J, V_g becomes 1.1235V and the following formula provides a good result[1], thus eliminating a trial and error time consuming for the initial guess of a_1:

$$a_1 = \frac{q\left(k_V - \frac{V_{0c}}{n_s T_{ref}}\right)}{kT_{ref}\left(\frac{k_I}{I_{pv}} - \frac{3}{T_{ref}} - \frac{E_g}{kT_{ref}^2}\right)} \tag{28}$$

The results for a_1 are summarized in Table 3, with a very good correlation between (25), (26) and (28). This is the reason we have adopted the Villalva value of 1.2034.

Table 3. Different a_1 values

a_1 **accepted range**	**Phang, equation (25)**	**De Blas, equation (26)**	**Saloux, equation (27)**	**Villalva, equation (28)**
1 – 1.5	1.1952	1.2016	1.6377	1.2034

[1] Formula (28) was adapted from [53], as the additional presence of the n_s in the initial formula provided correct results only for $n_s = 1$

Peer-reviewed version available at Energies 2018, 11, 36; doi:10.3390/en11010036

Xiao et al. [18] specify a linear decreases of the ideality factor with the temperature for the Shell ST40 module, ranging from 1.85 to 1.15, corresponding to 5 to 45 Celsius degree variance respectively. From the data plotted in their work, the following law can be adopted:

$$a_1 = 7.013 - 0.01875 \cdot T \tag{29}$$

Such approach must be taken with extreme care, as it is a common practice to operate often at temperatures higher than 48°C, where (29) yields $a_1 = 1$ (or 0 at 100°C)

De Soto at al. [20] come with a different proposal:

$$a_1 = a'_{1,ref} \frac{T}{T_{ref}} \tag{30}$$

which has a wrong slope. For a proper variation T and T_{ref} should be reversed as follows:

$$a_1 = a_{1,ref} \frac{T_{ref}}{T} \tag{31}$$

Our experiments presented in Figure 6 yielded a different result, closer to reversed Soto (31), according to the following linear dependency:

$$a_1 = 1.2512 - 0.002(T - 273.15) \tag{32}$$

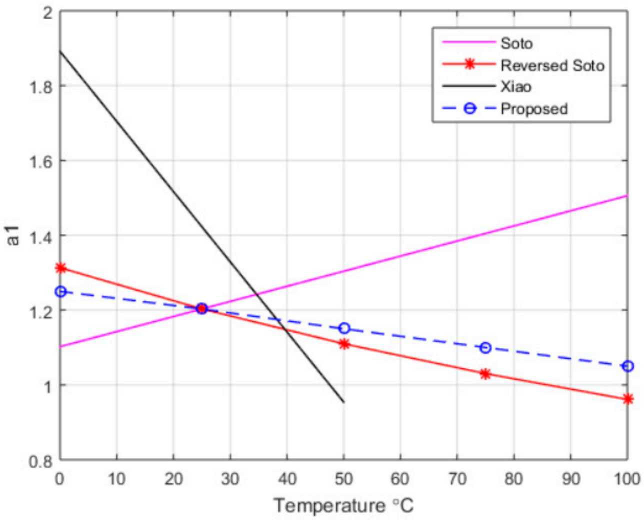

Figure 6. a_1 vs temperature

4.2.6. Selfheating Phenomenon

It is a common practice to express the internal cell temperature, T_{cell} based on Normal Operating Cell Temperature (NOCT) data, when the module is mounted 45° from horizontal.

$$T_{cell} = T_{amb} + (NOCT - 20)\frac{G}{800} \tag{33}$$

Here $G = 800\,{}^{\mathrm{W}}/_{\mathrm{m}^2}$, $T_{amb} = 20°\mathrm{C}$ and airflow is $1\ {}^{m}/_{s}$ [45].

The internal temperature of the PV was of permanent concern for the researchers [40 - 42], [46], but in most situations just an uncorrelated dependency is studied. Simply the temperature dependency of the I-V characteristic without acknowledging neither the real, actual temperature of the PV nor parameter variation is considered. Advanced simulators software packages include such features, MATLAB Simscape [52] being one of them.

In a recent work, Krac and Górecki [55] introduced a thermal model for the PV cell, where the self-heating is modeled. The thermal behavior is modeled by a thermal resistor and a thermal

Preprints (www.preprints.org) | NOT PEER-REVIEWED | Posted: 7 December 2017 doi:10.20944/preprints201712.0040.v1

Peer-reviewed version available at Energies 2018, 11, 36; doi:10.3390/en11010036

capacitor, a voltage source related to the ambient temperature and a current source that represents the total dissipated power within the PV. They claim that "for the maximum allowable value of the panel forward current (equal to 8 A), a self-heating phenomenon causes an increase in the panel temperature value equal only by 12°C." In our experiments, we acquired a rather extended influence, ranging from 20 to 30 °C.

Opposite to [54] and [55], the power dissipated by the PV cell is taken into account from the dissipative elements, which are resistive in our model. The energy flows from the two current sources to the resistors and the external circuit. Two or three current sources (or even diodes) are used in order to model different phenomena that take place inside the PV cell, the photoelectric effect and the behavior of p-n junction [8].

4.2.7. Open circuit voltage - V_{oc}

Ishaque and Salam [27] propose for the $V_{oc,cell}$ the following variation (34), which proves good correlation with the datasheet info and experimental data – see also Figure 7:

$$V_{oc,cell} = V_{0c,cell,ref} + a_1 \frac{kT}{q} ln \frac{G}{G_{ref}} + k_v \Delta T \tag{34}$$

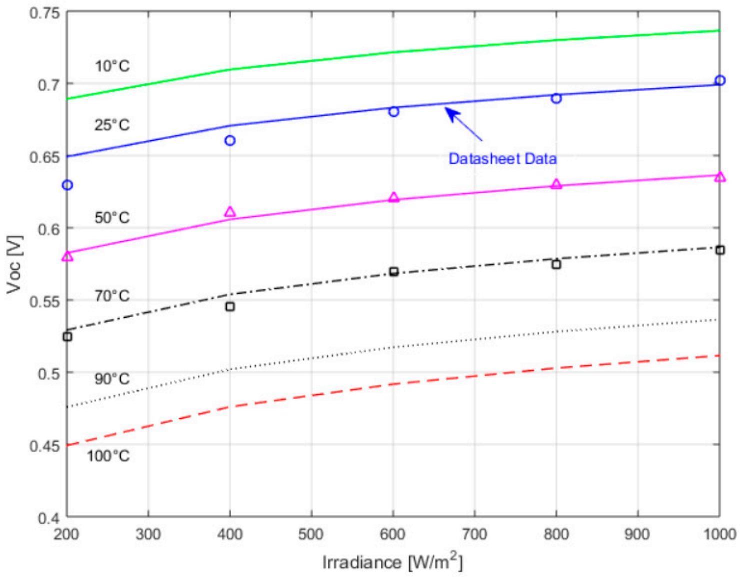

Figure 7. $V_{oc,cell}$ vs Irradiance for different temperatures. Solid and dashed lines are given by (33), while symbols correspond to experimental data.

Even (34) is not necessary for the model, it is another starting point for computing a_1.

4.3. The New Proposed PV Cell Model

The proposed model is presented in Figure 8. The upper section consists of standard elements, while the thermal modeling is ensured by the lower section. Here the current source labeled P_d simulates the power dissipated in the cell, the voltage labeled T_j is the cell temperature and the air temperature is modeled by the voltage source T_{amb}. The thermal resistance R_{th} models the thermal flow through the system structure, in our case the PV cell. The thermal capacitance C_{th} models the thermal inertia of the PV cell. Both R_{th} and C_{th} emulate all thermal transmission phenomena (conduction, convection and radiation) and depend of the materials, the finishing of the surfaces and on the mechanical dimensions of the system.

Peer-reviewed version available at Energies 2018, 11, 36; doi:10.3390/en11010036

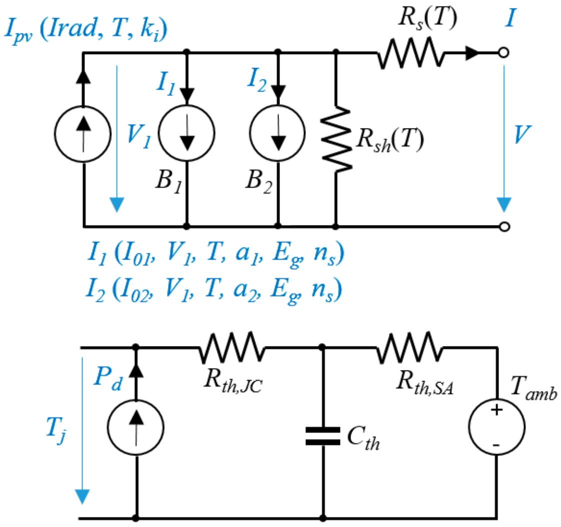

Figure 8. The new proposed electrical and thermal model of the PV cell.

The practical LTSpice model implementation is depicted in Figure 9. The upper circuit addresses the standard conditions (for reference and validation), while the middle section deals with the thermal model of the PV solar cell. The power associated with the circuit also includes the power due to the irradiance scaled with the cell area and the electrical power dissipated in R_s and R_{sh}.

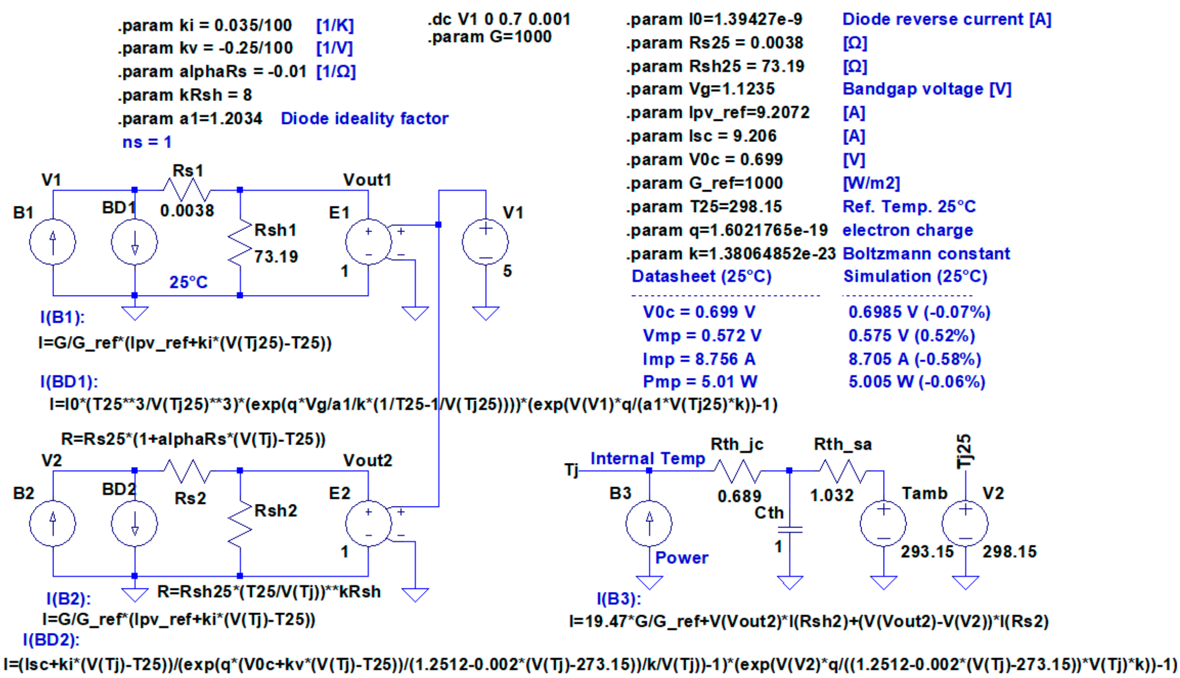

Figure 9. LTSpice PV Cell proposed model.

The thermal parameters R_{th} and C_{th} were extracted from experimental data. After a set of data was acquired, the temperature against time curve variation was fit and the time constant and the steady state value were determined. Unlike Górecki and Krac [54 - 56], we considered no dissipated power occurs in the BD2 current source of the model in Figure 9, as it makes no physical sense.

Preprints (www.preprints.org) | NOT PEER-REVIEWED | Posted: 7 December 2017 doi:10.20944/preprints201712.0040.v1

Peer-reviewed version available at *Energies* **2018**, *11*, 36; doi:10.3390/en11010036

5. Experimental Results

Figure 10 exhibits the simulated and the measured internal temperature of the PV cell and the dissipated power variation. It is worth mentioning that the corresponding NOCT for the temperature in Figure 9 is 47.2°C.

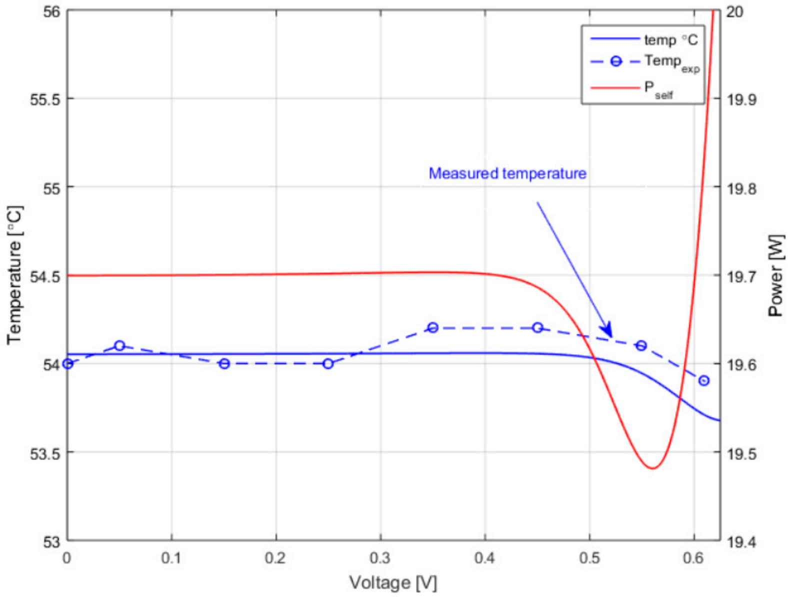

Figure 10. PV Cell dissipated power and temperature variation against voltage at STC.

Table 4 summarizes the main results for both the proposed model and the experiments performed for the PV cell. It can be observed that perfect agreement between the simulated and measured results is achieved.

Table 4. Comparison of the results at STC (25 Celsius, 1000 W/m2)

Symbol	Description	Datasheet Value	Proposed Model	Model Error vs Datasheet [%]	Experimental Values	
					Results	Error vs Datasheet [%]
$V_{oc,cell,ref}$	Cell open circuit voltage	0.699 V	0.6985 V	-0.07%	0.693 V	-0.86
$I_{sc,ref}$	Short circuit current	9.206 A	9.206A	0%	9.221 A	0.16
V_{mp}	Maximum power voltage	0.572 V	0.575 V	0.52%	0.569 V	-0.52
I_{mp}	Maximum power current	8.756 A	8.705 A	-0.58%	8.731 A	-0.29
(P_{mp})	Maximum power $P_{mp} = V_{mp} I_{mp}$	5.01 W	5.005 W	-0.06%	4.968 W	-0.81
FF	Fill factor	77.83%	77.84%	0.01%	77.52%	-0.40

The final validation of the model is presented in Figure 11 and Figure 12. Here the I-V and P-V characteristics of the PV cell are plotted at the reference temperature and at the operating temperature. Experimental data is represented with markers while the lines correspond to simulated results with the model proposed. A good correlation between the model and the experiments can be noticed.

Figure 12 (a) displays the serial resistance R_s influence on the output current and power. The solid lines graphs correspond to a fixed R_s while the dashed lines correspond to variable R_s with all the parameters included. At MPP a 98 mW power increase was observed. As estimated before, R_{sh} has a minor influence on the PV output – only 4.6 mW power decrease at MPP could be noticed, as displayed in Figure 12 (b). It is worth mentioning that in all cases the model self-computes the appropriate values for R_s and R_{sh}.

Peer-reviewed version available at *Energies* **2018**, *11*, 36; doi:10.3390/en11010036

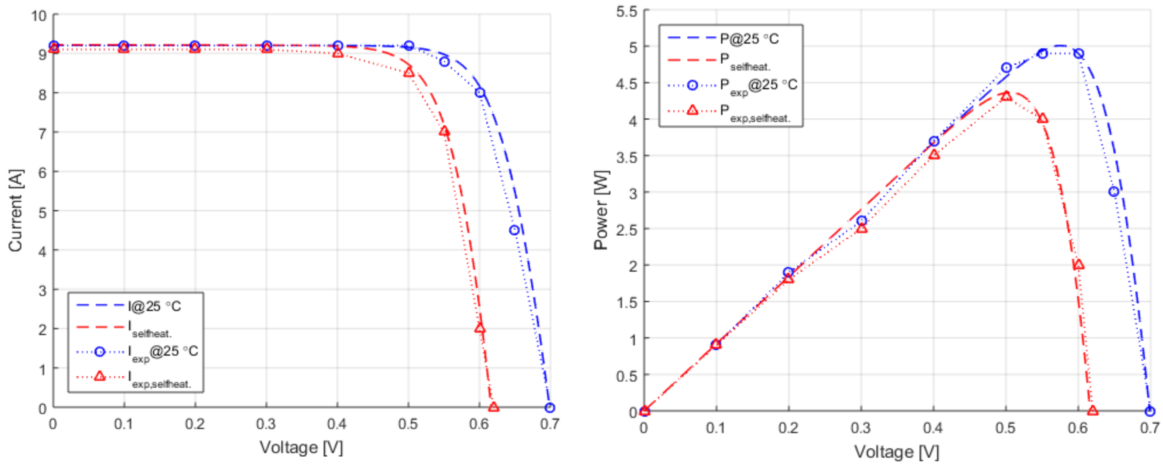

(a) (b)

Figure 11. I-V and P-V curves – simulation and experiments. (a) I-V curves at 25°C (upper lines) and with all parameters variation included (lower lines) – internal temperature is 54°C. (b) P-V curves at 25°C (upper lines) and with all parameters variation included (lower lines) – internal temperature is 54°C.

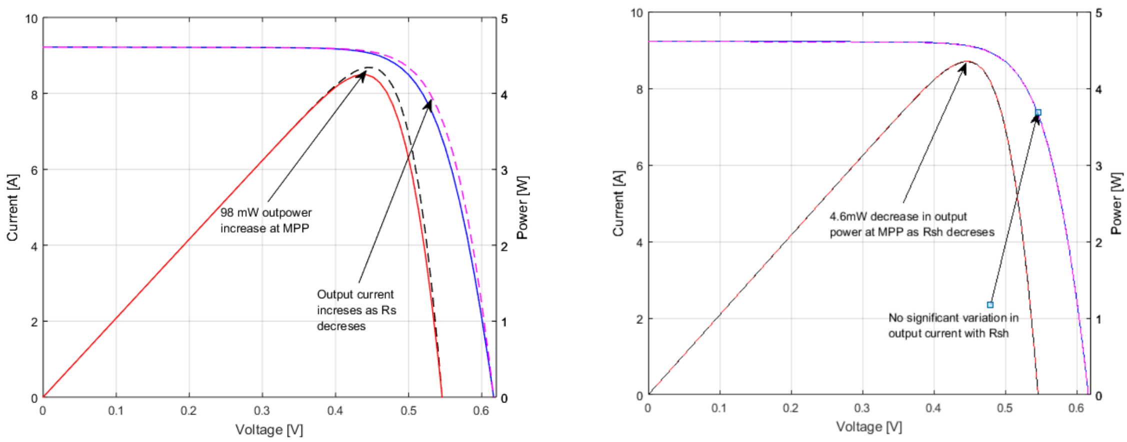

(a) (b)

Figure 12. R_s and R_{sh} influence and the performance. (a) R_s increase with temperature (25°C to 54°C) determines an increase in the output current and power (b) R_{sh} has no significant influence on the performance.

PV arrays compared (Table 5) were monocrystalline (Shell SP-70, MSMD290AS-36.EU and multycrystaline (Kyocera KG200GT, MSP300AS-36.EU, MSP290AS-36.EU, Sharp ND-224uC1)

Table 5. Datasheet available information for several commercial PV arrays

PV Type	n_s	V_{oc} $[V]$	V_{mp} $[V]$	I_{mp} $[A]$	I_{sc} $[A]$	k_V [mV/K]	k_I [mA/K]
Shell SP-70	36	21.4	16.5	4.24	4.7	-76	2
MSMD290AS-36.EU	72	44.68	37.66	7.7	8.24	-138.508	3.296
MSP290AS-36.EU	72	44.32	37.08	7.82	8.37	-146.256	3.348
KG200GT	54	32.9	26.3	7.61	8.21	-123	3.18
Sharp ND-224uC1	60	36.6	29.3	7.66	8.33	-131.76	4.4149

All the data from Table 5 was processed with the above proposed algorithm and the results are listed in Table 6, along with similar results from other researchers.

Peer-reviewed version available at Energies 2018, 11, 36; doi:10.3390/en11010036

Table 6. Comparison between previous solutions and our proposed model

PV Type	Solution	a_1	R_s [mΩ]	R_{sh} [Ω]	I_{pv} [A]	I_o [nA]
Shell SP-70	Ishaque* [35]	1&2.2	510	91	4.7	0.421;0.421
	Proposed	1.022	505	73.85	4.732	0.657
MSMD290AS-36.EU	Cubas [31]	1.1	130	316	8.24	2.36
	Proposed	1.0	159	194	8.247	0.243
MSP290AS-36.EU	Cubas [31]	1.1	162	331	8.37	2.86
	Proposed	1.02	191	230	8.377	0.513
KG200GT	Ishaque* [35]	1&2.2	320	160.5	8.21	0.422;0.422
	Sumathi et al. [5]	1.3	221	415.4	8.214	98.25
	Proposed	1.08	305	186	8.223	2.15
Sharp ND-224uC1	*Proposed*	1.06	316	108	8.354	1.41

* Ishaque at al. [35] use a 2 diode model with equal saturation currents

The final validation of the model was by applying the introduced model and computation method for the MSMD290AS-36.EU monocrystalline PV cell array and compare the results to the ones provided by Cubas et al. [31], as shown in Figure 13. As it can be seen, a good correlation exists between the two approaches.

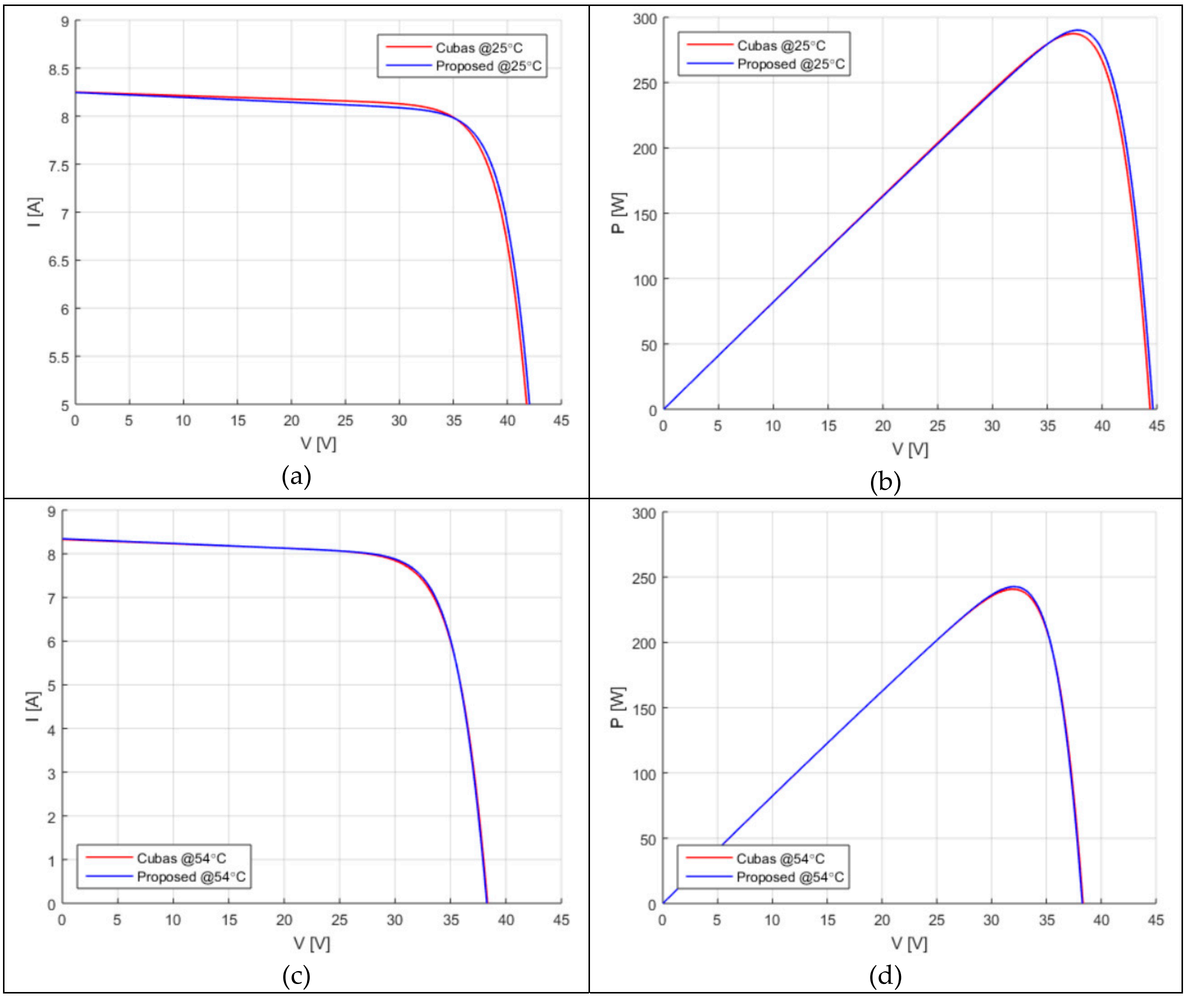

Figure 13. Final model validation by comparison for the MSMD290AS-36.EU monocrystalline PV cells. (a) I-V curves at 25°C; (b) P-V curves at 25°C (c) I-V curves at 54°C (d) P-V curves at 54°C.

6. Conclusions

A new thermo-electrical model for the PV cell was introduced. The model proved to be accurate, while considering parameter variation and selfheating phenomenon. Only free available tools were used during modeling. The literature analysis proved discrepancies between authors when studying parameter variation and proposals have been submitted.

As other authors have mentioned, R_{sh} influence is relatively reduced in the model. However a_1 proved to be a major factor. E_g displayed a small variance with temperature. Resistance R_s influence is important but sometimes shadowed by the wiring. The proposed model was accurately confirmed and validated by the experiments.

Acknowledgments: This work was supported by a grant of the Romanian National Authority for Scientific Research and Innovation, CNCS/CCCDI - UEFISCDI, project number PN-III-P2-2.1-PED-2016-0074, within PNCDI III.

Author Contributions: All of the authors have contributed to this research. Aurel Gontean conceived and designed the study. Aurel Gontean and Septimiu Lica carried out the simulation. Szilard Bularka performed the experiments. Dan Lascu analyzed the data. Aurel Gontean wrote the paper. Dan Lascu reviewed the manuscript. All authors read and approved the manuscript.

Conflicts of Interest: The authors declare no conflict of interest.

Nomenclature

Main Symbols	
a_1	Diode ideality factor
$a_{1,ref}$	Diode ideality factor at 25°C
R_{th}	Thermal capacitance of the cell, a lumped parameter
E_g	Bandgap energy
FF	Fill factor
G	Actual irradiance on cell surface
G_{ref}	Reference irradiance, 1000 W/m2
I	Solar cell current
I_{01}	Saturation current of the modeled diode, due to diffusion
$I_{01,ref}$	Saturation current of the modeled diode, due to diffusion, at 25°C
I_{mp}	Current at maximum power point
I_{pv}	Photo generated current
$I_{pv,ref}$	Photo generated reference current at 25°C
I_{sc}	Short circuit current of the solar cell
$I_{sc,ref}$	Short circuit current of the solar cell at 25°C
k	Boltzmann constant
k_I	Current temperature coefficient, A/K
k_V	Voltage temperature coefficient, V/K
k_P	Power temperature coefficient, W/K
$k_{R_s}, k_{R_{sh}}$	R_s, R_{sh} temperature exponent
k'_{Rs}, k'_{Rsh}	R_s, R_{sh} temperature exponent in Matlab
n_s	Number of series cells
n_p	Number of parallel cells
$P_{mp} = V_{mp} I_{mp}$	Maximum power
q	Electron charge
R_s	Cell series resistance
$R_{s,ref}$	Cell series resistance at 25°C
R_{s0}	Cell series resistance based on slope close to V_{oc}
R_{sh}	Cell parallel (shunt) resistance
$R_{sh,ref}$	cell parallel (shunt) resistance, at 25°C

Preprints (www.preprints.org) | NOT PEER-REVIEWED | Posted: 7 December 2017 doi:10.20944/preprints201712.0040.v1

Peer-reviewed version available at Energies 2018, 11, 36; doi:10.3390/en11010036

R_{sh0}	cell parallel (shunt) resistance based on slope close to I_{sc}
R_{th}	Thermal resistance of the cell, a lumped parameter
T	solar cell temperature, [K]
$T_{ref} = T_{25}$	reference temperature 298 K
$\Delta T = T - T_{ref}$	temperature difference
T_{amb}	ambient/air temperature, [°C]
T_{cell}	internal PV cell temperature, [°C]
V	solar cell voltage
V_{oc}	solar array open circuit voltage
$V_{oc,ref}$	solar array open circuit reference voltage at 25°C
$V_{oc,cell}$	solar cell open circuit voltage
$V_{oc,cell,ref}$	solar cell open circuit reference voltage at 25°C
V_{mp}	voltage at maximum power point
V_g	bandgap voltage
$V_T = kT/q$	diode thermal voltage

Abbreviations

AM	Air Mass
KCL	Kirchhoff's current law
MPP	Maximum power point
MPPT	Maximum Power Point Tracking
NOCT	Normal Operating Cell Temperature
PV	Photovoltaic
STC	Standard Test Conditions (cell temp. 25°C; irradiance 1000 W/m²; air mass 1.5)

Greek Symbols

α_{Rs}	series resistance temperature coefficient (linear law)

References

1. Rauschenbach, H.S., Solar Cell Array Design Handbook, *The Principles and Technology of Photovoltaic Energy Conversion*, Springer: New York, 1980; pp. 167-183, ISBN: 978-9401179171.
2. Patel, M. R., *Wind and Solar Power Systems*, CRC Press, 1999, pp. 32–48,137-157, ISBN: 0-8493-1605-7.
3. Emery, K., Measurement and Characterization of Solar Cells and Modules. In *Handbook of Photovoltaic Science and Engineering*, 2nd ed.; Luque, A., Hegedus S., Eds.; John Wiley & Sons: United Kingdom, 2011, pp. 1164, ISBN 978-0-470-72169-8, pp. 797–840.
4. Aparicio, M.P., Pelegrí-Sebastiá J., Sogorb T., Llario V., Modeling of Photovoltaic Cell Using Free Software Application for Training and Design Circuit in Photovoltaic Solar Energy. In *New Developments in Renewable Energy*, Arman H., Yuksel I., Eds., Intech: Vienna, Austria, 2013, pp. 121 – 139, ISBN 978-953-51-1040-8.
5. Sumathi, S., Kumar, L. A., Surekha, P., *Solar PV and Wind Energy Conversion Systems. An Introduction to Theory, Modeling with MATLAB/SIMULINK, and the Role of Soft Computing Techniques*, Springer: Switzerland, 2015, pp. 59-144, ISBN-13: 978-3319149400.
6. Khatib T., Elmenreich W., *Modeling of Photovoltaic Systems Using MATLAB: Simplified Green Codes*, John Wiley & Sons: Hoboken, New Jersey, US, 2016, pp. 39 - 88, ISBN-13: 978-1119118107.
7. Honsberg, C., Bowden, S., *Photovoltaic Education Network*, http://pveducation.org/pvcdrom/instructions, (accessed on 21 10 2017).
8. Van Zeghbroeck, B., *Principles of Semiconductor Devices*, https://ecee.colorado.edu/~bart/book/, 2011, (accessed on 21 10 2017).
9. LTSpice, http://www.linear.com/designtools/software/, (accessed on 21 10 2017).
10. Visual Studio Community, https://www.visualstudio.com/free-developer-offers/, (accessed on 21 10 2017).
11. S-Math Studio, https://en.smath.info/view/SMathStudio/summary/, (accessed on 21 10 2017).
12. Green, M. A., Solar cell fill factors: General graph and empirical expressions, *Solid State Electron* **1981**, *24(8)*, pp. 788 – 789, DOI 10.1016/0038-1101(81)90062-9.

Preprints (www.preprints.org) | NOT PEER-REVIEWED | Posted: 7 December 2017 doi:10.20944/preprints201712.0040.v1

Peer-reviewed version available at *Energies* **2018**, *11*, 36; doi:10.3390/en11010036

13. Phang, J.C.H., Chan, D.S.H., Phillips, J.R., Accurate Analytical Method For The Extraction Of Solar Cell Model Parameters, *Electron Lett* **1984**, *20(10)*, pp. 406 – 408, DOI: 10.1049/el:19840281.
14. Liu, G., Dunford, W.G., Photovoltaic Array Simulation, Proceedings of the ESA Sessions at 16th Annual IEEE PESC, Univ. Paul Sabatier, Toulouse, France, 24 – 28 June 1985, pp.145 - 153.
15. Gow, J.A., Manning, C.D., Development of a photovoltaic array model for use in power-electronics simulation studies, *IEE Proc. – El. Power App.* **1999**, 146(2), , pp. 193 – 200, DOI: 10.1049/ip-epa:19990116.
16. Walker, G., Evaluating MPPT converter topologies using a MATLAB PV model, *J Electr Electron Eng Aust* **2001**, *21(1)*, pp. 49 – 55.
17. De Blas, M.A., Torres, J.L., Prieto, E., Garcia, A., Selecting a suitable model for characterizing photovoltaic devices, *Renew Energy* **2002**, *25(3)*, pp. 371 – 380, DOI 10.1016/S0960-1481(01)00056-8.
18. Xiao W., Dunford, W.G., Capel, A., A Novel Modeling Method for Photovoltaic Cells, Proceedings of the 35th Annual IEEE Power Electronics Specialists Conference, 2004, pp. 1950 – 1956.
19. King D.L., Boyson, W.E., Kratochvill, J.A., Photovoltaic Array Performance Model, Sandia National Laboratories, December 2004, Available online: http://prod.sandia.gov/techlib/access-control.cgi/2004/043535.pdf, accessed on 21 10 2017.
20. De Soto, W., Klein, S.A., Beckman, W.A., Improvement and validation of a model for photovoltaic array performance, Sol Energy **2006**, *80(1)*, pp. 78 – 88, DOI: 10.1016/j.solener.2005.06.010.
21. Schlosser, V., Ghitas, A., Measurement of Silicon Solar Cells AC Parameters, Proceedings of the Arab Regional Solar Energy Conference (ARSEC 2006), University of Bahrain, Kingdom of Bahrain, 5–7 November 2006, pp. 1 – 15.
22. Villalva, M.G., Gazoli, J.R., Filho, E.R., Comprehensive Approach to Modeling and Simulation of Photovoltaic Arrays, *IEEE T Power Electr* **2009**, *24(5)*, pp. 1198 – 1208, DOI: 10.1109/TPEL.2009.2013862.
23. Kim, S.K., Jeon, J.H., Cho, C.H., Kim, E.S., Ahn, J.B., Modeling and simulation of a grid-connected PV generation system for electromagnetic transient analysis, *Sol Energy* **2009**, vol. 83 , pp. 664 – 678.
24. Di Piazza, M.C., Vitale, G., Photovoltaic field emulation including dynamic and partial shadow conditions, *Appl Energy* **2010**, *87(3)*, pp. 814 – 823, DOI: 10.1016/j.apenergy.2009.09.036.
25. Jung J.H., and S. Ahmed, Model Construction of Single Crystalline Photovoltaic Panels for Real-time Simulation, IEEE Energy Conversion Congress & Expo, September 12 – 16, 2010, Atlanta, USA.
26. Kim, W., Choi, W., A novel parameter extraction method for the one-diode solar cell model, *Sol Energy* 2010, *84(6)*, pp. 1008 – 1019, DOI: 10.1016/j.solener.2010.03.012.
27. Ishaque K., Salam Z., An improved modeling method to determine the model parameters of photovoltaic (PV) modules using differential evolution (DE), *Sol Energy* **2011**, *85(9)*, pp. 2349 – 2359, DOI: 10.1016/j.solener.2011.06.025.
28. Saloux, E., Teyssedoua, A., Sorin Mikhail, Explicit model of photovoltaic panels to determine voltages and currents at the maximum power point, *Sol Energy* **2011**, 85 (5), 2011, pp. 713 – 722, DOI: 10.1016/j.solener.2010.12.022.
29. Cuce, P.M., Cuce, E., A Novel model of photovoltaic modules for parameter estimation and thermodynamic assessment, *Int J Low Carbon Tech* **2011**, *7(2)*, pp. 159 – 165, DOI: 10.1093/ijlct/ctr034.
30. Tian, H., Mancilla-David, F., Ellis, K., Muljadi, E., Jenkins, P., A cell-to-module-to-array detailed model for photovoltaic panels, *Sol Energy* **2012**, Volume 86(9), pp. 2695-2706, DOI: 10.1016/j.solener.2012.06.004.
31. Cubas, J., Pindado, S., de Manuel, C., Explicit Expressions for Solar Panel Equivalent Circuit Parameters Based on Analytical Formulation and the Lambert W-Function, *Energies* **2014**, 7, pp. 4098 – 4115, DOI: doi:10.3390/ece-1-c013.
32. Aller, J., Viola J., Quizhpi, F., Restrepo, J., Ginart, A., Salazar, A., Implicit PV cell parameters estimation used in approximated closed-form model for inverter power control, Proceedings of the 2017 IEEE Workshop on Power Electronics and Power Quality Applications (PEPQA), Bogotá, Colombia, May 31-June 2017, pp. 1 – 6.
33. Chan, D., Phang J., Analytical Methods for the Extraction of Solar-Cell Single- and Double-Diode Model Parameters from I-V Characteristics, *IEEE Trans Electron Devices* **1987**, *34(2)*, pp. 286 – 293, DOI: 10.1109/T-ED.1987.22920.
34. Sandrolini, L., Artioli, M., Reggiani, U., Numerical method for the extraction of photovoltaic module double-diode model parameters through cluster analysis, *Appl Energy* **2010**, 87(2), pp. 442 – 451, DOI: 10.1016/j.apenergy.2009.07.022.

Preprints (www.preprints.org) | NOT PEER-REVIEWED | Posted: 7 December 2017 doi:10.20944/preprints201712.0040.v1

Peer-reviewed version available at *Energies* **2018**, *11*, 36; doi:10.3390/en11010036

35. Ishaque, K., Salam, Z., Syafaruddin, A comprehensive MATLAB Simulink PV system simulator with partial shading capability based on two-diode model, *Sol Energy* **2011**, *85(9)*, pp. 2217 – 2227, DOI: 10.1016/j.solener.2011.06.008.
36. Soon, J.J., Low, K.S., Goh, S.T., Multi-dimension diode photovoltaic (PV) model for different PV cell technologies, Proceedings of the IEEE 23rd International Symposium on Industrial Electronics (ISIE), Istanbul, Turkey, 2014, pp. 1 – 6.
37. Pandey, P.K., Sandhu, K.S., Multi Diode Modelling of PV Cell, Proceedings of the IEEE 6th India International Conference on Power Electronics (IICPE), National Institute of Technology Kurukshetra, India, 2014, pp. 1 – 4.
38. Erdem Z., Erdem, M.B., A Proposed Model of Photovoltaic Module in Matlab/SimulinkTM for Distance Education, *Procedia Soc Behav Sci* **2013**, *103*, 2013, pp. 55 – 62, DOI: 10.1016/j.sbspro.2013.10.307.
39. 156mm monocrystalline Mono solar cell 6x6, https://www.aliexpress.com/item/50pcs-lot-4-6W-156mm-mono-solar-cells-6x6-150feet-Tabbing-Wire-15feet-Busbar-Wire-1pc/1932804007.html, accessed on 21 09 2017.
40. Radziemska, E., Klugmann, E., Thermally affected parameters of the current–voltage characteristics of silicon photocell, *Energ Convers Manage* **2002**, *43(14)*, pp. 1889 – 1900, DOI: 10.1016/S0196-8904(01)00132-7.
41. Tsuno, Y., Hishikawa, Y., Kurokawa K., Temperature and Irradiance Dependence of the I-V Curves of Various Kinds of Solar Cells, Proceedings of the 15th International Photovoltaic Science & Engineering Conference PVSEC-15, Shanghai China, 2005, pp. 422 – 423.
42. Singh, P., Singh, S.N., Lal, M., Husain, M., Temperature dependence of I–V characteristics and performance parameters of silicon solar cell, *Sol Energ Mat Sol C* **2008**, *92(12)*, pp. 1611–1616, DOI: 10.1016/j.solmat.2008.07.010.
43. Cuce, E., Bali, T., Variation of cell parameters of a p-Si PV cell with different solar irradiances and cell temperatures in humid climates, Proceedings of the 4th International Energy and Environment Symposium, Sharjah, United Arab Emirates, April 19 – 23, 2009.
44. Ghani, F., Duke, M., Numerical determination of parasitic resistances of a solar cell using the Lambert W-function, *Sol Energy* **2011**, *85*, pp. 2386 – 2394, DOI: 10.1016/j.solener.2011.07.001.
45. Romary, F., Caldeira, A., Jacques, S., Schellmanns, A., Themal Modelling to Analyze the Effect of Cell temperature on PV Modules Energy Efficiency, Proceedings of the 14th European Conference on Power Electronics and Applications (EPE 2011), Birmingham, United Kingdom, 2011.
46. Wen, C., Fu, C., Tang, J. et al., The influence of environment temperatures on single crystalline and polycrystalline silicon solar cell performance, *Sci China Phys Mech Astron*, 2012, *55*, pp. 235 – 241, DOI: 10.1007/s11433-011-4619-z.
47. Cuce, E., Cuce, P.M., Bali, T., An experimental analysis of illumination intensity and temperature dependency of photovoltaic cell parameters, *Appl Energy* **2013**, *111*, pp. 374 – 382, DOI: 10.1016/j.apenergy.2013.05.025.
48. Bellia A.H., Ramdani, Y., Moulay, F., Medles, K., Irradiance And Temperature Impact On Photovoltaic Power By Design Of Experiments, *Rev Roum Sci Tech-El* 2013, 58(3), pp. 284–294.
49. Araneo, R., Grasselli, U., Celozzi, S., Assessment of a practical model to estimate the cell temperature of a photovoltaic module, *Int J Energy Environ* Eng **2014**, 5(2), pp, 1-16, DOI: 10.1186/2251-6832-5-2.
50. Chander, S., Purohit, A., et al., A study on photovoltaic parameters of mono-crystalline silicon solar cell with cell temperature, Energy Reports, vol. 1, 2015, pp. 104 – 109, DOI: 10.1016/j.egyr.2015.03.004.
51. Aller, J., Viola, J., et al., Explicit Model of PV Cells considering Variations in Temperature and Solar Irradiance, Proceedings of ANDESCON, Arequipa Peru, 2016, pp. 1 – 4.
52. Solar Cell Model, https://www.mathworks.com/help/physmod/elec/ref/solarcell.html, accessed on 10 08 2017.
53. Personal webpage Prof. Dr. Marcelo Gradella Villalva, https://sites.google.com/site/mvillalva/pvmodel, accessed on 21 09 2017.
54. Górecki, K., Górecki, P., Paduch, K., Modelling Solar Cells with Thermal Phenomena Taken into Account, *J. Phys.: Conf. Ser* **2014**, 494, 2014, pp. 1 – 8, DOI: 10.1088/1742-6596/494/1/012007.
55. Krac E., Górecki K., Modelling characteristics of photovoltaic panels with thermal phenomena taken into account, *IOP Conf. Ser.: Mater. Sci. Eng.* 2015, 104, 2015, pp. 1 – 7, DOI: 10.1088/1757-899X/104/1/012013.
56. Górecki, K., E. Krac, E., Measurements of thermal parameters of solar modules, *J. Phys.: Conf. Ser.* **2016**, *709*, pp. 1 – 6, DOI: 10.1088/1742-6596/709/1/012007.